

# Optical and magneto-optical resonances in nanocorrugated ferromagnetic films

M. V. Sapozhnikov,<sup>1,\*</sup> S. A. Gusev,<sup>1</sup> B. B. Troitskii,<sup>2</sup> and L. V. Khokhlova<sup>2</sup>

<sup>1</sup>*Institute for Physics of Microstructures, RAS, Nizhny Novgorod, GSP-105, Russia*

<sup>2</sup>*G.A.Razuvaev Institute of Organometallic Chemistry, RAS, Nizhny Novgorod, GSP-445 Russia*

\*Corresponding author: msap@ipm.sci-nnov.ru

Received June 8, 2011; revised August 22, 2011; accepted September 28, 2011;  
posted September 30, 2011 (Doc. ID 148943); published October 25, 2011

We report here on optical and magneto-optical spectra investigations of nanostructured Co and Ni films deposited on top of polymethyl methacrylate (PMMA) colloidal crystal. Resonant peculiarities have been observed in both spectra; their positions are scaled with the PMMA sphere diameter and depend on incident angle. Asymmetry of the resonance lineshapes as well as change of the direction of magneto-optical rotation has been observed. Both the surface plasmon resonance and the interference between reflections from the colloidal crystal and from the nanostructured film should be considered to explain the obtained results. © 2011 Optical Society of America

OCIS codes: 250.5403, 160.3820, 240.6680.

Since T. W. Ebbesen and co-workers found out extraordinary optical transmission through subwavelength holes [1] and explained it by resonance excitation of surface plasmon-polariton (SPP), the optics of nanostructures became a rapidly developing area. During the past two decades studies have been focused on noble metals nanostructures due to low absorption losses of the SPPs in these metals and due to their potential for possible applications [2,3]. The SPP effects become less pronounced in ferromagnetic materials due to the larger losses, but the plasmon excitations can influence their magneto-optic (MO) properties which recently have been predicted theoretically [4]. A very limited number of experimental works are devoted to study of the surface plasmon resonance (SPR) effects in noble metal/ferromagnetic composite structures [5,6], optical transmission through a subwavelength hole arrays in magnetic films [7–9], and of MO effects in magnetic periodic nanostructures [8–10]. Both resonant increase [9] and decrease of MO rotation were observed [8].

In this Letter we report on experimental studies of the optical and MO resonant properties of ferromagnetic films deposited on a surface of PMMA colloidal crystals. This system seems to be very promising material for plasmonics investigations [11] and besides it can be manufactured by relatively simple methods which do not require any expensive lithographic techniques.

Preparation of the colloidal crystals is based on self-assembly of monodisperse PMMA globules suspended in aqueous environment. 3D colloidal crystals have been obtained by means of drying of the suspension on a flat glass substrate in a chamber at room temperature. Thickness of the obtained colloidal crystal films is 100–300  $\mu\text{m}$ . The PMMA particles were synthesized by polymerization of MMA monomer in the water solution in presence of the potassium peroxodisulfate (0.08 wt.%). The ordered ferromagnetic nanostructures have been prepared by magnetron sputtering of a thin Co or Ni layer (10–60 nm) on the surface of the PMMA colloidal crystal. So the PMMA nanospheres have been hemispherically covered with metal and the fabricated ferromagnetic film has a strong 2D surface corrugation with a period dictated by the

template (290–410 nm in our experiments). Reference flat metal films have been deposited on a glass substrate in the same process. The morphology of the samples has been studied by scanning electron microscopy (SEM, Fig. 1(a)). The size of the colloidal crystal crystallites with different orientations of the crystal axes is 30–50  $\mu\text{m}$ .

The optical reflection spectra of the nanocorrugated and reference flat films have been measured for the incident angles in the range 20°–70° (hereafter measured from surface normal) both for *s* and *p* polarizations in the spectral range 280–1100 nm. The MO spectra have been measured in meridional configuration in the external fields up to 2000 Oe. The value of a Kerr signal is a difference between the polarization angles of the reflected light when a sample is magnetized to saturation in two opposite directions (denoted by arrows on the Fig. 2(b) inset). The following distinguished features have been found in the Kerr spectra of the nanocorrugated Co films: spectra have been lost a monotonic character, which is typical for flat Co films [Fig. 1(c)] and has two valleys. Let us define them as long-wave (LW) and short-wave (SW) minima. The typical shape of the Kerr spectra is represented on the Fig. 2. To understand the observed intriguing difference of MO properties between flat and nanostructured films we have investigated the

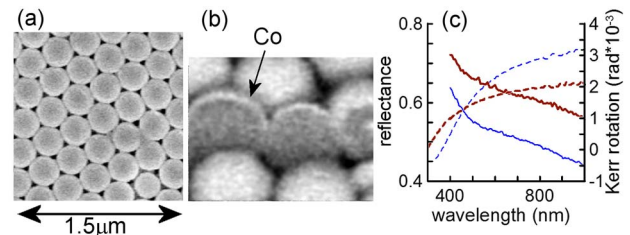


Fig. 1. (Color online) (a) SEM image of the 30 nm Co film on the top of the colloidal crystal (period 370 nm). (b) Microphotography of the particles cross-section made by focused  $\text{Ga}^+$  ion beam, the Co coverage is visible as bright layer. (c) Reflection coefficient (dashed lines) and Kerr rotation (solid lines) of the flat Co (red thick lines) and Ni (blue thin lines) films for 45° of the incident angle for *s*-polarization, the film thickness is 30 nm.

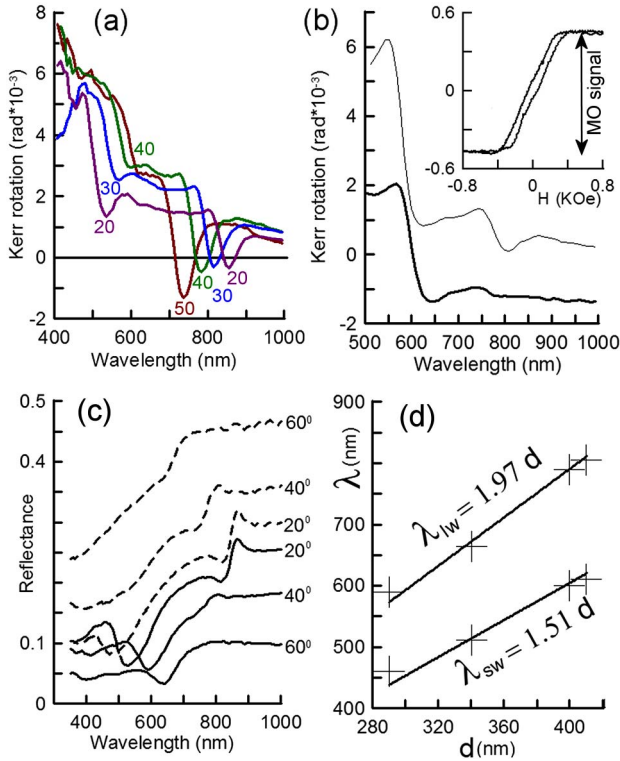


Fig. 2. (Color online) (a) Kerr rotation of 30 nm thick nanocorrugated Co film with the period 410 nm for  $p$ -polarization of the incident light and for 20°, 30°, 40° and 50° of incident angle. (b) Kerr rotation of 60 nm thick nanocorrugated Ni (thick line) and Co (thin line) films with the period 410 nm for  $p$ -polarized light incident at 40°, inset: typical magnetization curve. (c) Optical reflection spectra of 30 nm thick nanocorrugated Ni film with the period 370 nm for  $s$  (dashed lines) and  $p$ -polarization (solid lines) of the incident light and for different incident angles. (d) Scaling of the long-wave and short-wave minima in MO spectra of the nanocorrugated Co films with the period of the structure. Co thickness is 60 nm, the incident angle is 40°. Crosses are the experimental data, lines represents linear approximation.

spectra of nanocorrugated films with different periods and film thicknesses for various light polarizations and incident angles. The main results are summarized here:

- The shape of the spectra for  $s$ - and  $p$ -polarization of the incident angle is practically the same, although the valleys are more pronounced for  $p$ -polarization.
- The LW-minimum blue-shifts as the incident angle increases in the same manner for  $s$ - and  $p$ -polarizations. On the contrary, the SW-minimum red-shifts in the same conditions, [Fig. 2(a)–2(c)].
- The MO spectra of nanocorrugated films are scaled with a colloidal particle diameter which determined the period of the structure. Both the positions of LW- and SW-minima show monotonous red-shift as the structure period increases [Fig. 2(d)].
- With the increase of the film thickness up to 60 nm, the LW-minimum become less pronounced, while the SW-minimum remain unchanged [Fig. 2(b)].
- Quite often one or both minima become so deep, that the direction of the polarization rotation even changes its sign [Fig. 2(a)].

The other series of the samples have been prepared using Ni as ferromagnetic metal. The MO spectra of the nanocorrugated Ni films demonstrate the appearance of the same two valleys and have the same dependence on experimental parameters as in the case of the Co films. The typical shape of the spectrum is represented on the Fig. 2(b) for the 60 nm nanocorrugated Ni film. The figure also demonstrates the fact, that the LW-minimum become less pronounced in the case of the thick films. The main differences between Co and Ni samples is related to the fact that even in the case of flat Ni films the coefficient of the Kerr rotation is less than in the case of Co films. In addition, it changes its sign at approximately 800 nm [Fig. 1(c)].

The measurements of mirror reflection spectra [Fig. 2(c)] of the nanocorrugated Co and Ni films show their complete identity for different light polarizations and incident angles. The reason for such similarities, obviously, is the fact that dielectric constants of these materials are very similar in magnitude in the optical range [12]. Both reflection spectra have two peculiarities that are strongly correlated with the positions of the MO spectra valleys. Comparing the positions of valleys in the Kerr spectra (which are more pronounced) with the peculiarities in reflection spectra, it becomes evident that LW peculiarity in the reflection spectra is not a simple valley but has an asymmetric lineshape.

Let us try to elucidate the physical mechanisms which can lead to such spectra shapes. As in the case of periodically perforated metallic films, the SPP can be excited by incident light, thereby leading to the spectral structure. The dispersion of the resonance with the incident angle and the scaling of the spectra with the period of the structure are the fingerprints of the SPP excitations. In the case of the 2D corrugation, the SPP can be excited both by  $s$ - and  $p$ -polarization of the incident light. In hexagonally corrugated structure, the SPPs are excited under the condition of  $k_{\text{SPP}} = k_0 + G_{m,n}$ , where  $k_0$ ,  $k_{\text{SPP}}$ , and  $G_{m,n} = 4\pi(mi + mj)/(3^{1/2}d)$  are the wavevectors of the incident light along the film plane, the SPP wavevector and the hexagonal lattice reciprocal vector respectively,  $d$  is the structure period. For estimations we have used the simplest approximation of SPPs on the flat surface with the dispersion relation  $k_{\text{SPP}} = \omega/c(\epsilon_m\epsilon_d/(\epsilon_m + \epsilon_d))^{1/2}$ . Here  $\epsilon_d$  is the permittivity of dielectric and it is equal to 1 or 2.25 for air or PMMA,

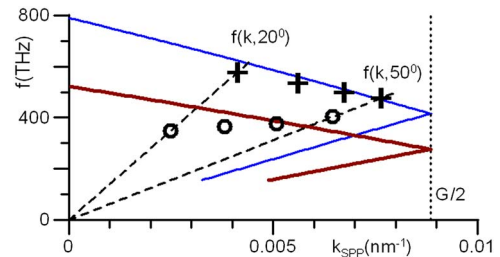


Fig. 3. (Color online) The dispersion curves for SPP calculated for Co-air interface (thin blue line) and for Co-PMMA interface (thick red line) in the first Brillouin zone (denoted by dotted line) for the structure with the period of 410 nm. The dashed lines denoted the dispersion lines for the light incident at 20° and 50°. Crosses and circles are the experimental data for the SW and LW resonances correspondingly.

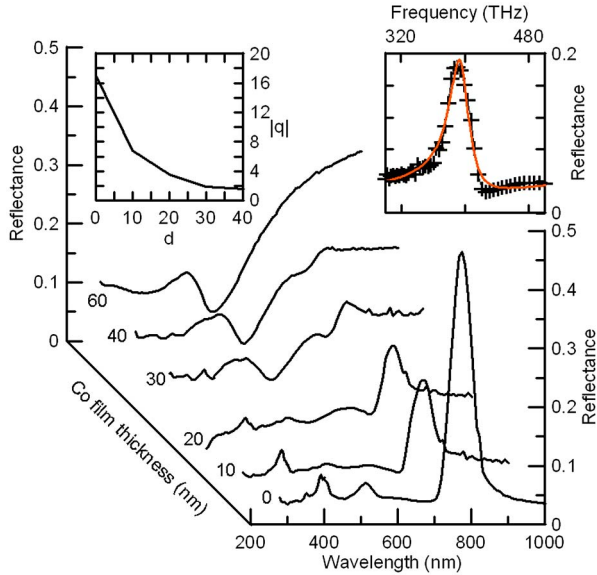


Fig. 4. (Color online) Dependence of the reflection spectrum on the Co film thickness ( $p$ -polarized light incident at  $40^\circ$ , the structure with 410 nm period). (a) Inset represents the dependence of the measured Breit–Wigner–Fano coupling coefficient  $q$  on the film thickness. (b) Inset is a sample of Fano fit for 10 nm thick nanocorrugated Co film.

correspondingly.  $\epsilon_m$  is the permittivity of metal film, in our estimations we have used the data for Co and Ni permittivity from [13]. Actually, we found a good agreement between the measured SW-resonance positions and the calculated positions for  $[\pm 1, 0]$  SPP resonance for metal-air interface (Fig. 3) even in this simplest model. Decrease in the Kerr rotation and even change of its sign near the resonance can be explained on the basis of the same SPR. Probably the angle of Kerr rotation in the reflectance channel connected with the SPP excitation has the sign opposite to MO rotation at the nonresonant reflection. In this case, if the contribution of SPR channel to the reflection is significant enough, then there is a change in the Kerr rotation sign. The similar effects were observed in the hexagonal lattice of Co antidotes [9].

While the estimation shows that LW peculiarities of the spectra are in the same frequency range where SPP on the Co-PMMA interface should be, its dispersion is determined by a position of Bragg peak in the reflection of the colloidal crystal substrate. So LW peculiarity blueshifts with the angle. The initially symmetric Bragg resonance lineshape in the reflection of the colloidal crystal becomes more and more asymmetric as the deposited film thickness increases (Fig. 4). The asymmetry of the lineshape is the result of interference of two reflection processes: the resonant Bragg reflection from the 3D colloidal crystal and the reflection from the nanocorrugated film, so the Fano model is appropriate. For an

isolated Fano resonance, the reflection lineshape can be written as  $R_{\text{Fano}} = R_0 + R_a(\epsilon_\nu + q)^2/(1 + \epsilon\nu^2)$ , where  $\epsilon_\nu = (\omega - \omega_\nu)/(\Gamma/2)$ .  $R_0$  is a slowly varying reflectance;  $R_a$  is a contribution of a zero-order continuum state that couples with the discrete resonant state.  $\omega_\nu$  and  $\Gamma$  are peak frequency and linewidth of the resonant state, respectively, and  $q$  is the coupling coefficient, characterizing the ratio between resonant and nonresonant reflection. Using the Fano model fit to our data we have found out that the  $|q|$  decreases from  $\sim 20$  to 1.5 as the deposited film increases up to 40 nm, which corresponds to decrease of the role of the Bragg reflection from colloidal crystal substrate [12]. With the further increase of the film, the resonance becomes less pronounced as the film become less transparent.

In summary, we experimentally found the resonance peculiarities in the reflection and Kerr rotation spectra of the 2D nanocorrugated magnetic films on the top of PMMA colloidal crystal. The positions of resonances are scaled with the period of corrugation and have dispersion with the angle. The spectral peculiarities are attributed to the surface plasmon resonance excitation and to the interference between reflections from the colloidal crystal substrate and from the nanostructured film.

This research was supported by Russian Foundation for Basic Research (RFBR), Russian Federation (RF) Agency for Education (Rosobrazovanie), and RF Agency for Science and Innovation.

## References

1. T. W. Ebbesen, H. J. Lezec, H. F. Ghaemi, T. Thio, and P. A. Wolff, *Nature* **391**, 667 (1998).
2. P. Neuzil and J. Reboud, *Anal. Chem.* **80**, 6100 (2008).
3. E. Ozbay, *Science* **311**, 189 (2006).
4. A. Zharov and V. V. Kurin, *J. Appl. Phys.* **102**, 123514 (2007).
5. T. V. Murzina, I. A. Kolmychek, A. A. Nikulin, E. A. Gan'shina, and O. A. Aktsipetrov, *JETP Lett.* **90**, 504 (2009).
6. C. Clavero, K. Yang, J. R. Skuza, and R. A. Lukaszew, *Opt. Lett.* **35**, 1557 (2010).
7. F. Przybilla, A. Degiron, J.-Y. Laluet, C. Genet, and T. W. Ebbesen, *J. Opt. A* **8**, 458 (2006).
8. M. Diwekar, V. Kamaev, J. Shi, and Z. V. Vardeny, *Appl. Phys. Lett.* **84**, 3112 (2004).
9. G. Cstistis, E. Papaioannou, P. Patoka, J. Gutek, P. Fumagalli, and M. Giersig, *Nano Lett.* **9**, 1 (2009).
10. Z. Liu, L. Shi, Z. Shi, X. H. Liu, J. Zi, S. M. Zhou, S. J. Wei, J. Li, X. Zhang, and Y. J. Xia, *Appl. Phys. Lett.* **95**, 032502 (2009).
11. C. Farcau and S. Astilean, *J. Opt. A* **9**, S345 (2007).
12. A. E. Miroshnichenko, S. Flach, and Y. S. Kivshar, *Rev. Mod. Phys.* **82**, 2257 (2010).
13. P. B. Johnson and R. W. Christy, *Phys. Rev. B* **9**, 5056 (1974).